# Time-Domain Waveform Synthesis Using a Dual-Polarization Modulator

Fangzheng Zhang, *Member, IEEE*, Bindong Gao, and Shilong Pan, *Senior Member, IEEE*

***Abstract*— This letter proposes a time-domain waveform synthesis based on a dual-polarization modulator that is driven by single-frequency radio frequency signals. This is achieved by applying a dual-polarization modulator to generate a polarization multiplexed optical signal. By controlling the parameters of the driving signals, multiple waveforms can be generated by synthesizing optical intensity profiles along two orthogonal polarization states. Compared with previously reported signal generators, the proposed time-domain waveform synthesizer is simple, compact, and easy to implement. The generation of triangular, flat-top, and sawtooth pulse trains with 5- and 10-GHz repetition rates are demonstrated in this letter. The results indicate that the proposed system is feasible and would find applications in optical signal processing and microwave photonic signal processing systems.**

***Index Terms*— Waveform synthesis, microwave photonics, polarization multiplexing.**

## I. Introduction

MICROWAVE waveform generators are widely used in modern communication, radar and instrumentation systems. The traditional electrical signal generators, such as a direct digital synthesizer (DDS), have limited bandwidth that cannot meet the requirements in electrical systems working at high frequency band and requiring a large bandwidth. To address this problem, photonic-assisted microwave signal generation has been proposed, having the advantages of high frequency, large bandwidth and immunity to electromagnetic interference [1], [2]. One such method is implemented by Fourier synthesis [3]. Using this method, arbitrary waveforms can be generated by properly processing the optical spectrum. Another photonic arbitrary waveform generation method is realized by optical spectral shaping and frequency-to-time mapping [4]–[6]. In this method, the waveform is generated by reshaping the spectrum of short optical pulse trains and converting the spectral profiles into time domains using chromatic dispersion. An optical spectrum processor is required for both these methods. Photonic-assisted microwave signal generation can also be implemented by external modulation of a continuous wave (CW) light. The basic theory is to generate a series of sidebands through nonlinear electro-optical modulation, and then manipulate the amplitude and phase of these modulation harmonics to attain a specific waveform in time-domain. Typically, in addition to the electro-optical modulator in such systems, other optical devices are required to manipulate the optical sidebands. For example, using a dual-drive Mach-Zehnder modulator (MZM) together with a span of dispersion fiber, versatile signals including short pulses, flat-top pulses, triangular pulses and sawtooth pulses are generated [7]. In another example, a polarization modulator placed inside a Sagnac loop can generate triangular, sawtooth and square pulses [8].

The previously mentioned photonic waveform generators are implemented by frequency-domain synthesis. Alternatively, photonic signal generators by time-domain synthesis have also been proposed. An example of this is the photonic digital-to-analog converter (PDAC), which can generate arbitrary waveforms by performing digital-to-analog conversion based on photonic techniques [9]. Despite the great flexibility, a PDAC usually has a complicated structure and a poor bit-resolution, preventing commercial applications. Recently, another time-domain waveform synthesis method was proposed [10], which temporally synthesized the optical waveforms carried by two wavelengths. This method demonstrates good performance but the system is complicated due to multiple laser sources and modulators being required. Furthermore, a span of fiber is needed to introduce a proper time delay between the two channels.

In this letter, we propose a new time-domain waveform synthesis method using a dual-polarization modulator. The dual-polarization modulator is used to generate a polarization multiplexed signal. By controlling the radio frequency (RF) driving signals as well as the bias voltages applied to the modulator, various waveforms can be generated by temporally synthesizing the optical intensities of the polarization multiplexed signal. The prominent feature of the proposed waveform synthesizer is the ability to generate multiple waveforms with a very simple and compact structure, which only requires a laser source, an integrated modulator and a single-frequency RF source. In the experimental demonstration, periodical triangular, flat-top and sawtooth pulses are successfully generated.

## II. Principle and Simulation

Fig. 1 shows the setup of the proposed signal generator. The key component is a dual-polarization modulator that consists of two MZMs (MZM1 and MZM2), a polarization rotator (PR) and a polarization beam combiner (PBC). When the CW light

Manuscript received June 2, 2016; revised September 15, 2016; accepted October 1, 2016. Date of publication October 6, 2016; date of current version October 31, 2016. This work was supported in part by the NSFC Program under Grant 61401201, Grant 61422108, and Grant 61527820, in part by the NSFC Program of Jiangsu Province under Grant BK20140822, in part by the Aviation Science Foundation of China under Grant 2015ZC52024 and Grant 2013ZC52050, in part by the Jiangsu Planned Projects for Postdoctoral Research Funds under Grant 1302074B, in part by the Postdoctoral Science Foundation of China under Grant 2015T80549 and Grant 2014M550290, and in part by the Fundamental Research Funds for Central Universities.

The authors are with the Key Laboratory of Radar Imaging and Microwave Photonics, Ministry of Education, Nanjing University of Aeronautics and Astronautics, Nanjing 210016, China (e-mail: pans@ieee.org).

Color versions of one or more of the figures in this letter are available online at http://ieeexplore.ieee.org.

Digital Object Identifier 10.1109/LPT.2016.2615126

1041-1135 © 2016 IEEE. Personal use is permitted, but republication/redistribution requires IEEE permission.
See http://www.ieee.org/publications_standards/publications/rights/index.html for more information.

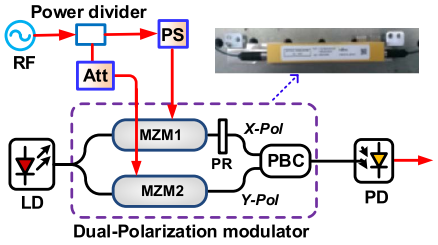


Fig. 1. The schematic diagram of the proposed triangular pulse generator. LD: laser diode; PBC: polarization beam combiner; MZM: Mach-Zendher modulator; PS: electrical phase shifter; Att: electrical power attenuator; PD: photodetector.

generated from a laser diode (LD) is sent to the modulator, it is split equally into two branches. The light in each branch is modulated by an MZM, respectively. Then, the polarization of the signal in the upper branch is rotated by 90 degree by the PR. Thus, a pair of orthogonally polarized ($X$-pol and $Y$-pol) optical signals are obtained in the two branches. After they are combined at the PBC, a polarization multiplexed optical signal is acheived. In the proposed system, the two MZMs are driven by two RF signals from the same RF source. The phase difference between the two driving signals can be adjusted by a phase shifter (PS). The amplitude of each driving signal can be controlled by tuning the power of the RF source and adjusting the electrical power attenuator. Mathematically, the intensity waveforms of the signals in $X$-pol and $Y$-pol are described by:

$$I_{X-pol}(t) = \frac{I_0}{4}\left[1+\cos\left(\frac{A_1\pi}{V_\pi}\cos(2\pi f t)+\frac{\pi V_{DC1}}{V_\pi}\right)\right] \quad (1)$$

$$I_{Y-pol}(t) = \frac{I_0}{4}\left[1+\cos\left(\frac{A_2\pi}{V_\pi}\cos(2\pi f t+\Delta\varphi)+\frac{\pi V_{DC2}}{V_\pi}\right)\right] \quad (2)$$

where $I_0$ is the power of the light source, $V_\pi$ is the half-wave voltage of the two MZMs, $f$ is the RF frequency, $A_1$ and $A_2$ are the RF amplitudes, $\Delta\varphi$ is the phase delay between the two driving signals, and $V_{DC1}$ and $V_{DC2}$ are the bias voltages of MZM1 and MZM2, respectively. At the output of the dual-polarization modulator, the optical intensity profile is the time-domain synthesis of the waveforms in $X$ and $Y$ polarizations, which can be expressed as:

$$\begin{aligned} I(t) &= I_{X-pol}(t)+I_{Y-pol}(t) = \frac{I_0}{2}+\frac{I_0}{4} \\ &\times\left\{\begin{aligned} &\cos\left(\tfrac{\pi V_{DC1}}{V_\pi}\right)\left[J_0\left(\tfrac{A_1\pi}{V_\pi}\right)+2\sum_{n=1}^{\infty}(-1)^n \times J_{2n}\left(\tfrac{A_1\pi}{V_\pi}\right)\cos(4n\pi f t)\right] \\ &+\sin\left(\tfrac{\pi V_{DC1}}{V_\pi}\right)\left[2\sum_{n=1}^{\infty}(-1)^n J_{2n-1}\left(\tfrac{A_1\pi}{V_\pi}\right) \times \cos[(4n-2)\pi f t]\right] \\ &+\cos\left(\tfrac{\pi V_{DC2}}{V_\pi}\right)\left[J_0\left(\tfrac{A_2\pi}{V_\pi}\right)+2\sum_{n=1}^{\infty}(-1)^n \times J_{2n}\left(\tfrac{A_2\pi}{V_\pi}\right)\cos(4n\pi f t+2n\Delta\varphi)\right] \\ &+\sin\left(\tfrac{\pi V_{DC2}}{V_\pi}\right)\left[2\sum_{n=1}^{\infty}(-1)^n J_{2n-1}\left(\tfrac{A_2\pi}{V_\pi}\right) \times \cos[(4n-2)\pi f t+(2n-1)\Delta\varphi]\right] \end{aligned}\right. \end{aligned} \quad (3)$$

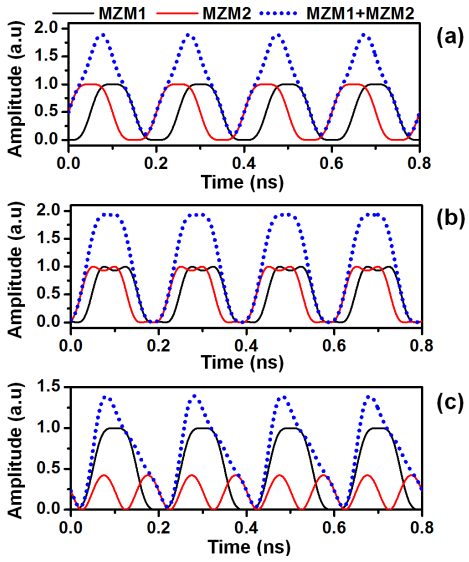


Fig. 2. Simulation results for generating triangular, flat-top and sawtooth pulses with a repetition rate of 5 GHz.

where $J_n$ denotes the $n$th order of the first kind Bessel function. When this optical signal is sent to a photodetector (PD), the waveform can be converted into electrical domain. By accurately setting the parameters ($A_1$, $A_2$, $V_{DC1}$, $V_{DC2}$, and $\Delta\varphi$), various waveforms can be generated. For the generation of a specific waveform, one can use the multivariable control method to search the possible values of the five variables. First, a target waveform is proposed. Then, initial values and search ranges of the variables are assigned. By substituting the initial values into Eq. (3), a waveform is generated. After that, the properties (i.e., waveform linearity and power spectrum) of the generated waveform and those of the target waveform are compared. If the difference is outside of a specified range, the variables are changed one by one for another round of waveform generation and comparison. Once the comparison result is within the specified range, the values of the variables are recorded. After all the variables within the searching ranges have been tested, the recorded variable values are checked again and an optimum waveform is obtained. No recording indicates that the target waveform cannot be generated by the proposed system.

In this letter, we demonstrate the generation of triangular, flat-top and sawtooth pulses. Fig. 2 shows the simulation results generating these waveforms. In all the cases, the RF frequency is 5 GHz and the generated pulses have a repetition rate of 5 GHz. For triangular pulse generation, MZM1 and MZM2 are biased at the quadrature point ($V_{DC1} = V_{DC2} = V_\pi/2$), and $A_1 = A_2 = 1.51$. After MZM1 and MZM2, two quasi-square optical pulse trains are generated (Fig. 2(a)). When $\Delta\varphi$ is equal to $\pi/2$, the combined optical waveform is a triangular pulse train. In this case, according to Eq. (3), the intensity of the combined optical signal is calculated to be (only the 1st- and 3rd-order harmonics are considered):

$$I(t) \propto DC+\cos\left(2\pi f t-\frac{3\pi}{4}\right)+\frac{1}{9}\cos\left[\cos 3\left(2\pi f t-\frac{3\pi}{4}\right)\right] \quad (4)$$

which agrees with the Fourier expansion of a triangular pulse train when harmonics higher than the 3rd-order are neglected [11]. Fig. 2(b) shows the results for flat-top pulse generation. When the two MZMs are biased at $0.45V_\pi$, and $A_1 = A_2 = V_\pi/2$, the generated optical pulses have slight power ripples at the top. If $\Delta\varphi$ is set to $\pi/4$, the power ripples in the two waveforms are complementary to each other, and the combined power profile has a flat-top. Here, the difference between the flat-top pulse and the quasi-square pulse generated by a single MZM is that the flat-top pulse has a larger pulse width and is more flat. For sawtooth pulse generation, MZM1 is biased at the quadrature point and MZM2 is biased at the minimum transmission point ($V_{DC1} = V_\pi/2$, $V_{DC2} = V_\pi$). The driving signal amplitudes are both $V_\pi/2$ ($A_1 = A_2 = V_\pi/2$). In this case, a quasi-square optical pulse train and a frequency doubled pulse train is generated after MZM1 and MZM2, respectively (Fig. 2(c)). When $\Delta\varphi$ is equal to $\pi/4$, the output waveform is close to a sawtooth shape.

## III. Experiment Results and Discussion

In the experiment, a CW light at 1550.51 nm is generated from an LD with a power of 13 dBm. The modulator is a dual-polarization BPSK (DP-BPSK) $LiNbO_3$ modulator (Fujitsu FTM7980) which has a 3 dB bandwidth of ~30 GHz and a $V_\pi$ of 3.5 V@ 21.5 GHz. The insertion loss of the modulator is about 10 dB when the two sub-MZMs are biased at the quadrature point. The RF signal is generated by a microwave signal generator (Keysight 5183N). The signal is first amplified by an electrical amplifier and then split into two branches by a power divider. An electrical phase shifter is used in one branch to adjust the phase difference, and a power attenuator is placed in the other branch to tune the power. The optical waveform is observed through an 80 GHz optical sampling oscilloscope (Agilent 86100C). After the modulator, a PD with a bandwidth of 20 GHz and a responsivity of 0.65 A/W is used to perform an optical-to-electrical conversion. The electrical spectrum is observed by an electrical spectrum analyzer (R&S FSV40). To analyze the optical waveform in each polarization, the signal from the DP-BPSK modulator is passed through a polarization controller (PC) and a polarization beam splitter (PBS). By accurately controlling the PC, the polarization multiplexed signals can be separated at the two output ports of the PBS.

Firstly, the RF frequency is set to be 5 GHz. Fig. 3 shows the measured optical waveforms when generating triangular pulses. After properly setting the power of the driving signals and the bias voltages, two quasi-square optical pulse trains are generated in $X$ and $Y$ polarizations, as shown in Fig. 3(a) and (b), respectively. By tuning the phase shifter to introduce a phase difference of $\pi/2$, the output waveform from the DP-BPSK modulator is a triangular pulse train (Fig. 3(c)). Fig. 4 shows the electrical spectrum of the generated 5 GHz triangular pulse train. The 10 GHz component is well suppressed and the power ratio between the 5 GHz and the 15 GHz components is 18.7 dB. Accordingly, the power of the 5 GHz component is about nine times that of the 15 GHz component, which is in agreement with Eq. (4).

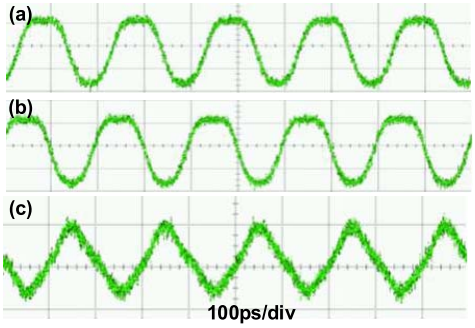


Fig. 3. Triangular pulse generation: (a), (b) are the measured waveforms in $X$-pol and $Y$-pol, and (c) is the generated 5 GHz triangular pulse train.

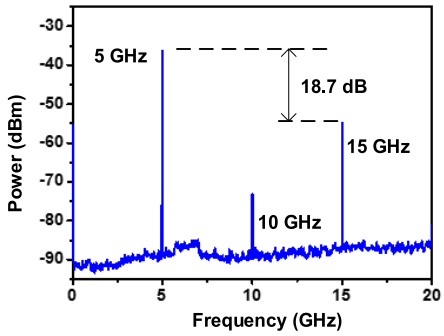


Fig. 4. Electrical spectrum of the 5 GHz triangular pulse train.

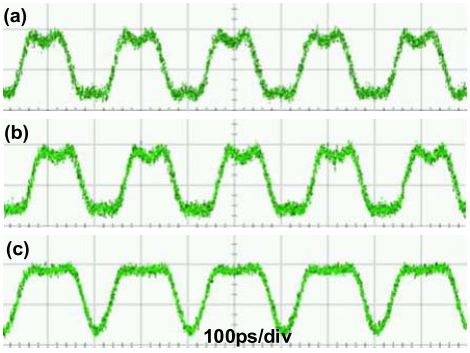


Fig. 5. Flat-top pulse generation: (a), (b) are the measured waveforms in $X$-pol and $Y$-pol, and (c) is the generated 5 GHz flat-top pulse train.

Fig. 5 shows the experimental results for flat-top pulse generation. Fig. 5(a) and (b) is the optical pulse train in $X$ polarization and $Y$ polarization, respectively. Apparent power ripples appear at the top of the pulses. By setting the phase delayed to $\pi/4$, the synthesized waveform after the DP-BPSK modulator is a 5 GHz flat-top pulse train. As shown in Fig. 5(c), the generated pulse has a very flat top that occupies more than 50% of a temporal period. Compared with the quasi-square pulse generated by a single MZM (Fig. 3(a)), the flat-top pulse in Fig. 5(c) has a broader pulse width and a greater flatness.

The results for generating sawtooth pulses are shown in Fig. 6. In $X$ polarization, a quasi-square optical pulse train is generated (Fig. 6(a)). A frequency doubled pulse train is generated in $Y$ polarization (Fig. 6(b)). After accurately setting the

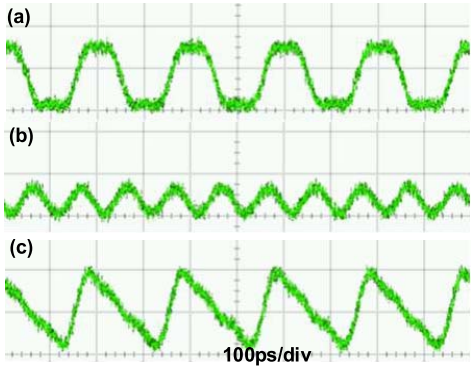


Fig. 6. Sawtooth pulse generation: (a), (b) are the measured waveforms in $X$-pol and $Y$-pol, and (c) is the generated 5 GHz sawtooth pulse train.

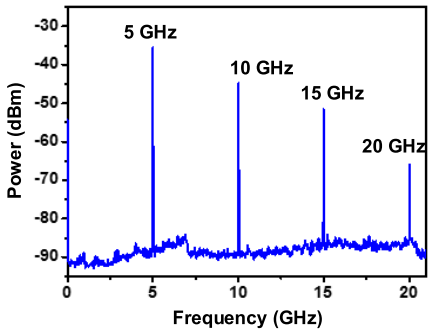


Fig. 7. Electrical spectrum of the 5 GHz sawtooth pulse train.

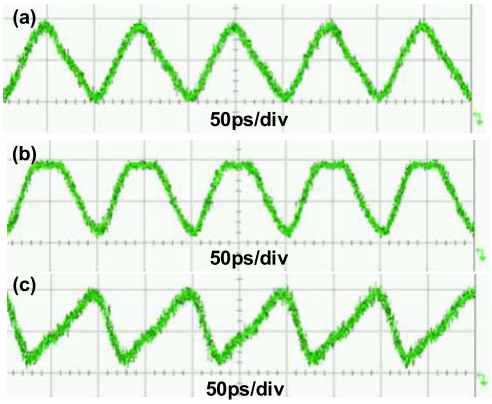


Fig. 8. The generated 10 GHz pulse trains: (a) triangular pulse trian, (b) flat-top pulse train and (c) sawtooth pulse train.

phase difference between the two RF signals, a sawtooth pulse train is obtained after the DP-BPSK modulator (Fig. 6(c)). The electrical spectrum of the sawtooth pulse train is measured (Fig. 7). Due to the limited bandwidth of the PD, only the 1st-, 2nd-, 3rd- and 4th-order harmonics are included. It can be concluded that the spectral power distribution in Fig. 7 is close to that of a sawtooth pulse train [8].

In this proposed system, the repetition rate of the generated waveform can be adjusted by changing the RF frequency. Fig. 8 shows the waveforms of the generated triangular, flat-top and sawtooth pulse trains with a repetition rate of 10 GHz. No waveform distortion is observed, differing from the 5 GHz pulses. Due to the hardware limitations (mainly the bandwidth of the PD), the generation of optical pulses with higher repetition rate is not observed. However, Fig. 8 suggests that the repetition rate can be refined in the proposed system. The stability of the generated waveform is an issue in the proposed system as it may be affected by the bias drift of the modulator. However, after the dual-polarization modulator reaches a steady-working state, the waveform appears to be very stable in the experiment.

## IV. Conclusion

We propose and demonstrate a time-domain waveform synthesizer that can generate various waveforms. The proposed system has a very simple structure, using a single laser source and a single modulator. The repetition rate of the generated waveforms can be refined. In the experimental demonstration, triangular, flat-top and sawtooth pulses with 5 GHz and 10 GHz repetition rates are successfully generated. The encouraging results indicate that this method has potential applications in future communication, radar and instrumentation systems.

## References

[1] J. Yao, "Photonic generation of microwave arbitrary waveforms," *Opt. Commun.*, vol. 284, no. 15, pp. 3723–3736, 2011.
[2] A. M. Weiner, "Ultrafast optical pulse shaping: A tutorial review," *Opt. Commun.*, vol. 284, no. 15, pp. 3669–3692, 2011.
[3] Z. Jiang, C. Huang, D. E. Leaird, and A. M. Weiner, "Optical arbitrary waveform processing of more than 100 spectral comb lines," *Nature Photon.*, vol. 1, no. 8, pp. 463–467, 2007.
[4] J. Chou, Y. Han, and B. Jalali, "Adaptive RF-photonic arbitrary waveform generator," *IEEE Photon. Technol. Lett.*, vol. 15, no. 4, pp. 581–583, Apr. 2003.
[5] J. Ye *et al.*, "Photonic generation of triangular-shaped pulses based on frequency to time conversion," *Opt. Lett.*, vol. 36, no. 8, pp. 1458–1460, Apr. 2011.
[6] Y. Li, A. Dezfooliyan, and A. M. Weiner, "Photonic synthesis of spread spectrum radio frequency waveforms with arbitrarily long time apertures," *J. Lightw. Technol.*, vol. 32, no. 20, pp. 3580–3587, Oct. 15, 2014.
[7] B. Dai, Z. Gao, X. Wang, H. Cheng, N. Kataoka, and N. Wada, "Generation of versatile waveforms from CW light using a dual-drive Mach-Zehnder modulator and employing chromatic dispersion," *J. Lightw. Technol.*, vol. 31, no. 1, pp. 145–151, Jan. 1, 2013.
[8] W. Liu and J. Yao, "Photonic generation of microwave waveforms based on a polarization modulator in a Sagnac loop," *J. Lightw. Technol.*, vol. 32, no. 20, pp. 3637–3644, Oct. 15, 2014.
[9] J. Liao, H. Wen, X. Zheng, H. Zhang, and B. Zhou, "A time-domain photonic arbitrary waveform generator," *Opt. Exp.*, vol. 20, no. 11, pp. 12631–12639, May 2012.
[10] Y. Jiang *et al.*, "Photonic microwave waveforms generation based on time-domain processing," *Opt. Exp.*, vol. 23, no. 15, pp. 19442–19452, Jul. 2015.
[11] F. Zhang, X. Ge, and S. Pan, "Triangular pulse generation using a dual-parallel Mach–Zehnder modulator driven by a single-frequency radio signal," *Opt. Lett.*, vol. 38, no. 21, pp. 4491–4493, Nov. 2013.